

# Conventional MRI and MR Angiography of Stroke

## Contents

<b>6.1</b>	<b>Conventional MRI and Stroke</b>	115
6.1.1	Hyperacute Infarct	115
6.1.2	Acute Infarct	117
6.1.3	Subacute Infarct	117
6.1.4	Chronic Infarcts	118
6.1.5	Hemorrhagic Transformation	119
6.1.6	Conclusion	120
<b>6.2</b>	<b>MR Angiogram and Stroke</b>	120
6.2.1	Noncontrast MRA	122
6.2.1.1	TOF MRA	122
6.2.1.2	Phase-Contrast MRA	124
6.2.2	Contrast-Enhanced MRA	126
6.2.3	Image Processing	126
6.2.4	Extracranial Atherosclerosis and Occlusions	127
6.2.5	Intracranial Atherosclerosis and Occlusions	130
6.2.6	Dissection	130
6.2.7	Other Infarct Etiologies	132
6.2.7.1	Moya Moya	132
6.2.7.2	Vasculitis	132
6.2.7.3	Fibromuscular Dysplasia	133
6.2.8	Venous Infarct	133
6.2.9	Conclusion	134
<b>References</b>		134

Stroke can be evaluated with both conventional MRI and MR angiography (MRA) sequences. The first section of this chapter discusses the appearance of stroke on conventional MR sequences (i.e., not diffusion or perfusion), while the second section discusses MRA and its role in evaluating stroke etiologies.

## 6.1 Conventional MRI and Stroke

Strokes have a characteristic appearance on conventional MRI that varies with infarct age. Temporal evolution of strokes is typically categorized into hyperacute (0–6 h), acute (6–24 h), subacute (24 h to approximately 2 weeks), and chronic stroke (>2 weeks old).

### 6.1.1 Hyperacute Infarct

In the hyperacute stage of infarct, there is occlusion or slow flow in the vessels supplying the area of infarcted tissue. Within minutes of the infarct, the signal flow void on T2-weighted images is lost (Fig. 6.1). FLAIR (fluid attenuated inversion recovery), an inversion recovery sequence that suppresses the CSF signal, can show high intravascular signal against the surrounding low-signal subarachnoid space [1] (Fig. 6.2). In one study, 65% of infarcts <6 h old showed a FLAIR high signal within vessels, and, in some cases, the finding of a FLAIR high signal in vessels preceded changes in the diffusion-weighted images [2].

Gradient recalled echo (GRE) T2\*-weighted images can detect an intraluminal thrombus (deoxyhemoglobin) in hyperacute infarcts as a linear low signal region of magnetic susceptibility (Fig. 6.2). In one

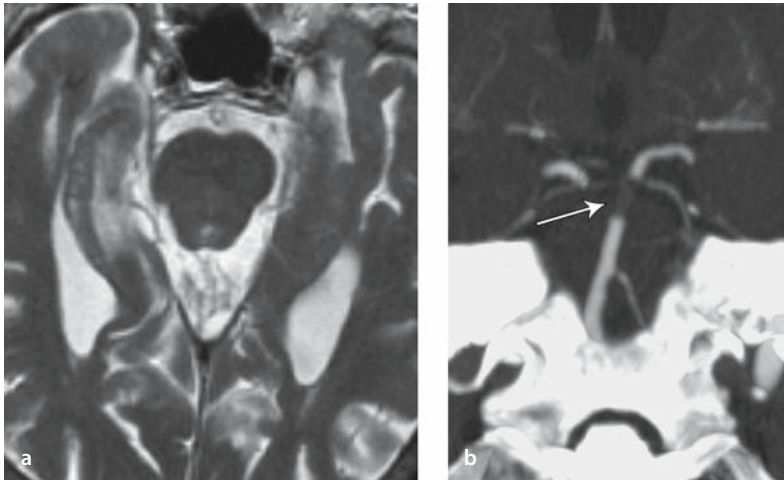


Fig. 6.1 a, b

Basilar occlusion. **a** The T2-weighted image shows loss of the signal flow void in the basilar artery in this patient with basilar occlusion and hyperacute pontine infarct. No parenchymal abnormality is noted at this early time point. **b** Coronal maximal intensity projection (MIP) image from the CT angiogram demonstrates the occlusion as a filling defect (arrow)

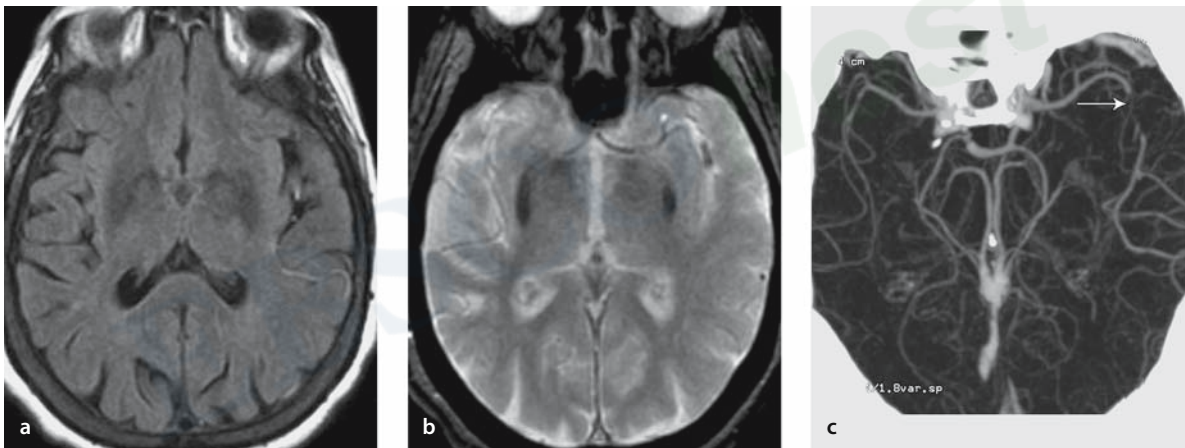


Fig. 6.2 a–c

Left middle cerebral artery (MCA) thrombus. The left MCA shows high signal from an intraluminal clot on FLAIR-weighted images (**a**) but low signal on gradient recalled echo (GRE) T2\*-weighted images (**b**). This corresponds to a filling defect (arrow) on CT angiogram (**c**). A subtle FLAIR high signal is present at the left insula

study of 30 patients with MCA thrombus, gradient echo had 83% sensitivity in detecting the thrombus, compared with 52% sensitivity for noncontrast CT in detecting a dense MCA sign [3].

Contrast-enhanced T1-weighted images show arterial enhancement in 50% of hyperacute strokes [1] (Fig. 6.3). This arterial enhancement is thought to be secondary to slow flow, collateral flow or hyperperfu-

sion following early recanalization. It may be detected as early as 2 h after stroke onset and can persist for up to 7 days. During this period, there is usually no parenchymal enhancement because inadequate collateral circulation prevents contrast from reaching the infarcted tissue. Rarely, early parenchymal enhancement may occur when there is early reperfusion or good collateralization.

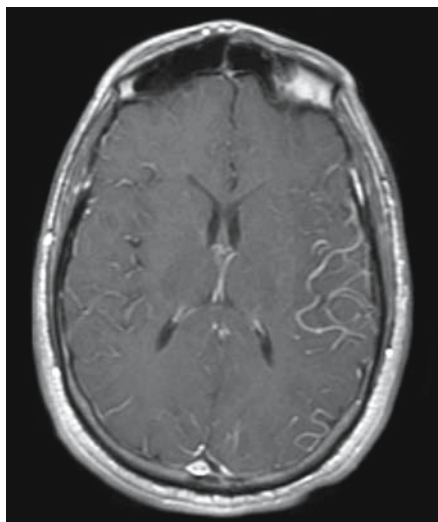


**Figure 6.3**

Arterial enhancement from infarct. T1-weighted post-contrast image shows increased enhancement of the left middle cerebral artery (MCA) vessels in this hyperacute infarct

In the hyperacute period (first 6 h), there is shift of water from the extracellular to the intracellular space but there may be little increase in overall tissue water. Therefore, while the development of altered signal intensity on FLAIR- or T2-weighted images may occur as early as 2–3 h after stroke onset, conventional MRI is not sensitive enough for evaluation of infarcts in the hyperacute stage; one study found an 18% sensitivity of T2-weighted images in detecting infarct in the first 6 h and a false-negative rate of 30–50% [4]. FLAIR-weighted sequences are slightly more sensitive than T2-weighted images in the detection of parenchymal changes in acute infarcts but have an estimated sensitivity of only 29% in the first 6 h [5].

### 6.1.2 Acute Infarct

By 24 h, as the overall tissue water content increases due to vasogenic edema following blood–brain barrier disruption, conventional MRI becomes more sensitive for the detection of parenchymal infarcts. Signal changes during the first 24 h are best appreciated

in the cortical and deep gray matter. Infarcts in the acute stage usually demonstrate focal or confluent areas of T2 and FLAIR hyperintensity with sulcal effacement. During this time, the white matter may be hyperintense, but also may show no abnormality or demonstrate hypointensity. Proposed etiologies for the subcortical white matter hypointensity are free radicals, sludging of deoxygenated red blood cells, and iron deposition [6]. Because cerebrospinal fluid (CSF) is hypointense, FLAIR has improved detection of small infarctions in brain parenchyma, such as cortex and periventricular white matter, adjacent to CSF. By 24 h, T2-weighted and FLAIR-weighted images detect 90% of infarcts [1]. An increase in tissue water also leads to hypointensity on T1-weighted images. However, in the acute period, T1-weighted images are relatively insensitive at detecting parenchymal changes compared with T2-weighted images. At 24 h, sensitivity is still only approximately 50%.

### 6.1.3 Subacute Infarct

In the subacute phase of infarct (1 day to 2 weeks), the increase in vasogenic edema results in increased T2 and FLAIR hyperintensity, increased T1 hypointensity, and better definition of the infarction and swelling (Fig. 6.4). The brain swelling is manifest as gyral thickening, effacement of sulci and cisterns, effacement of adjacent ventricles, midline shift, and brain herniation. The swelling reaches a maximum at about 3 days and resolves by 7–10 days [7]. There is increased T2 and FLAIR signal within the first week that usually persists but there may be “MR fogging” [8]. MR fogging occurs when the infarcted tissue becomes difficult to see because it has developed a signal intensity similar to that of normal tissue. This is thought to result from infiltration of the infarcted tissue by inflammatory cells. One study of 7- to 10-day-old strokes identified 88% of subacute strokes on T2-weighted images, and another determined that T2- and FLAIR-weighted images were equally sensitive at detecting 10-day-old infarcts [7].

In the subacute phase, arterial enhancement peaks at 1–3 days. Large infarcts will also demonstrate meningeal enhancement that may represent reactive

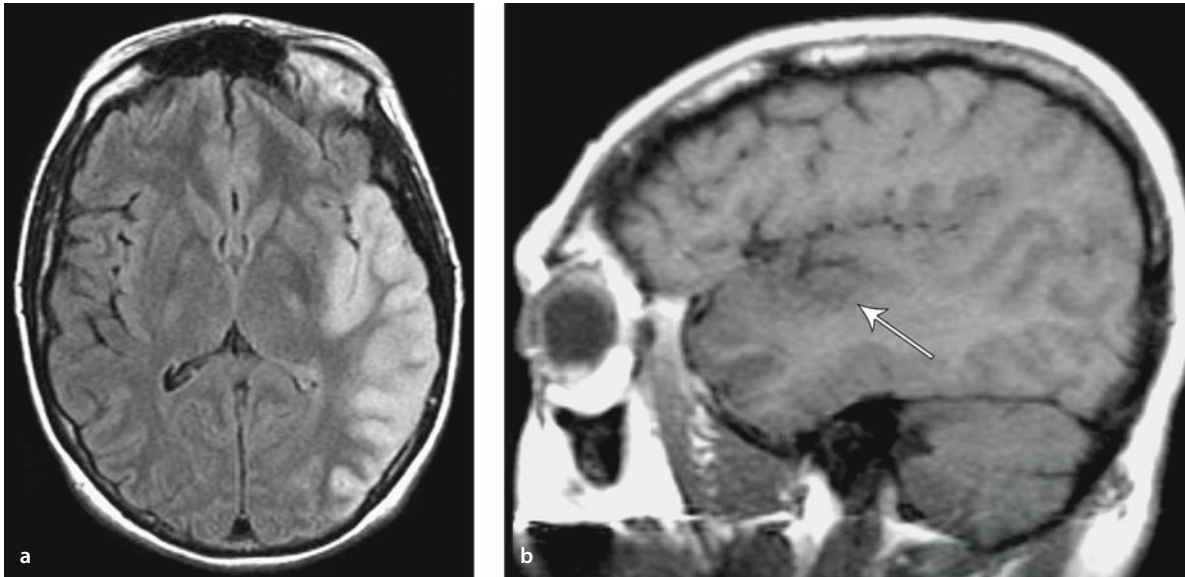


**Fig. 6.4 a, b**

Cortical edema in a subacute infarct. **a** The axial FLAIR-weighted image shows high signal, gyral swelling, and sulcal effacement. **b** There is subtle low signal and gyral swelling (arrow) seen on the T1-weighted sagittal image

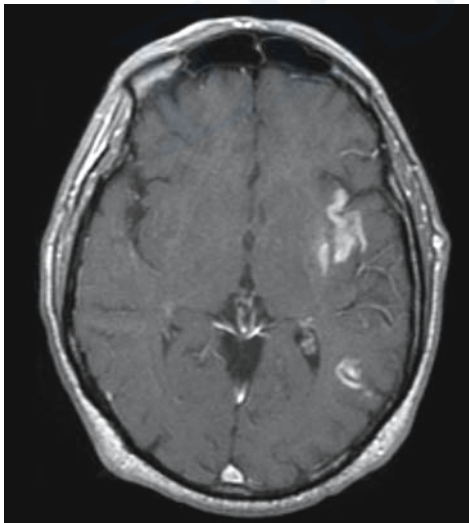


**Figure 6.5**

Enhancing infarcts. Postcontrast T1-weighted image shows gyriform enhancement at the left insula and posterior parietal lobe from a subacute left MCA infarct

hyperemia, which peaks at 2–6 days. Arterial and meningeal enhancement both typically resolve by 1 week [9]. In addition, parenchymal enhancement occurs during this phase. Gray matter enhancement can appear band-like or gyriform (Fig. 6.5). This is secondary to disruption of the blood–brain barrier and restored tissue perfusion from a recanalized occlusion or collateral flow. This parenchymal enhancement may be visible at 2–3 days but is consistently present at 6 days and persists for 6–8 weeks [9]. Some infarcts, such as watershed and noncortical infarcts, may enhance earlier.

#### 6.1.4 Chronic Infarcts

After 2 weeks, the mass effect and edema within infarcts decrease and the parenchyma develops tissue loss and gliosis. During this time, parenchymal enhancement peaks at 1–4 weeks and then gradually fades [9]. The chronic stage of infarction is well es-

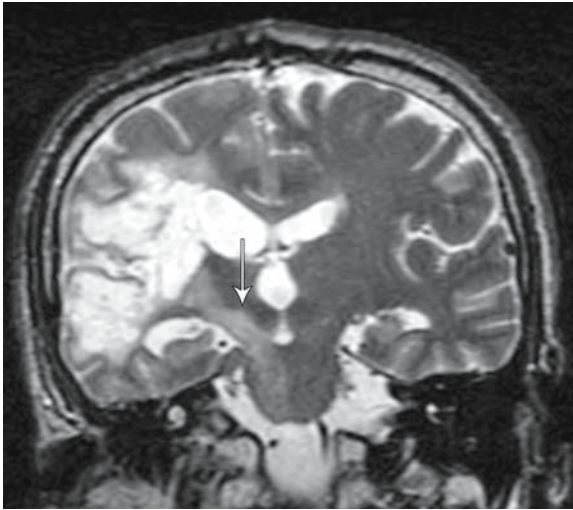


Figure 6.6

Wallerian degeneration. Coronal T2-weighted image shows encephalomalacia of the right frontal and temporal lobes and T2 high signal extending into the right cerebral peduncle (arrow) from Wallerian degeneration

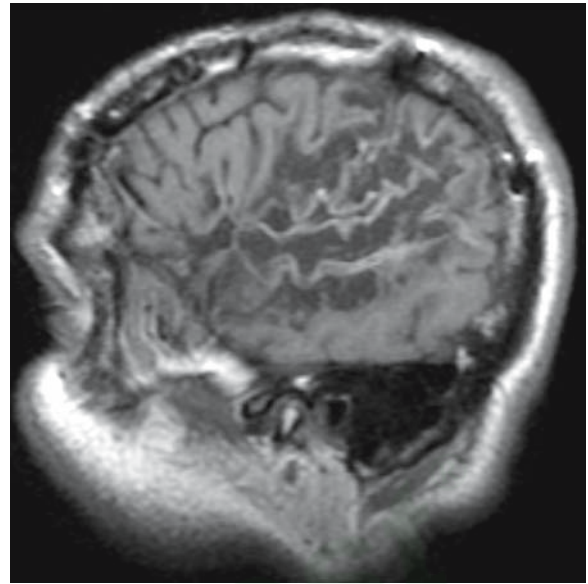


Figure 6.7

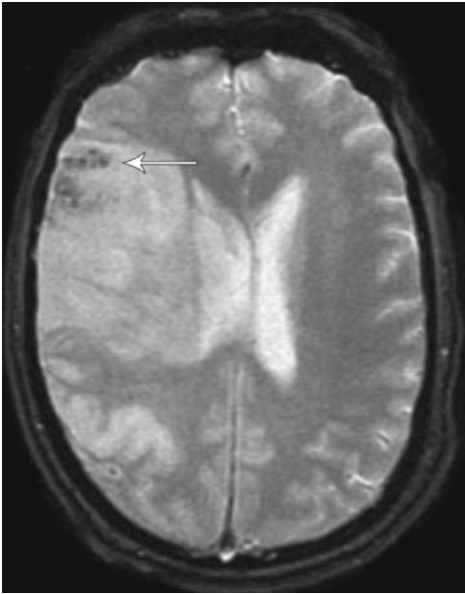
Laminar necrosis. This sagittal noncontrast T1-weighted image shows gyriform T1 high signal in a chronic left MCA infarct. Mild enlargement of the sulci is consistent with encephalomalacia

established by 6 weeks. At this point, necrotic tissue and edema are resorbed, the gliotic reaction is complete, the blood–brain barrier is intact, and reperfusion is established [9]. There is no longer parenchymal, meningeal or vascular enhancement, and the vessels are no longer hyperintense on FLAIR images. There is tissue loss with ventricular, sulcal, and cisternal enlargement. There is increased T2 hyperintensity and T1 hypointensity due to increased water content associated with cystic cavitation. With large middle cerebral artery (MCA) territory infarctions, there is Wallerian degeneration, characterized by T2 hyperintensity and tissue loss, of the ipsilateral cortical spinal tract [10] (Fig. 6.6).

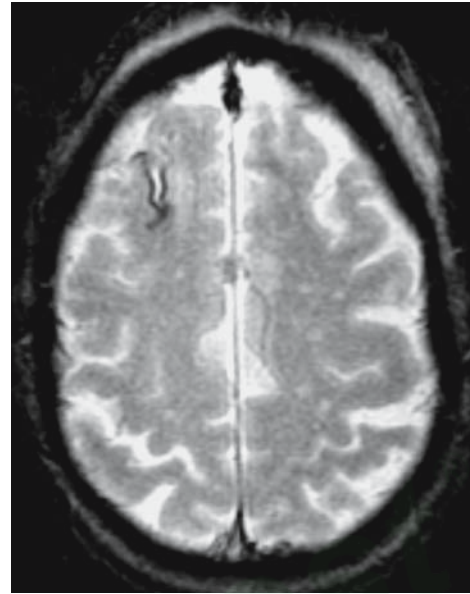
Chronic infarcts can demonstrate peripheral gyriform T1 high signal from petechial hemorrhage or from laminar necrosis [11] (Fig. 6.7).

### 6.1.5 Hemorrhagic Transformation

Hemorrhagic transformation (HT) of brain infarction represents secondary bleeding into ischemic tissue, varying from small petechiae to parenchymal hematoma. It has a natural incidence of 15% to 26% during the first 2 weeks and up to 43% over the first month after cerebral infarction [12, 13]. Predisposing factors include stroke etiology (HT is more frequent with embolic strokes), reperfusion, good collateral circulation, hypertension, anticoagulant therapy, and thrombolytic therapy. In patients treated with intra-arterial (i.a.) thrombolytic therapy, a higher National Institutes of Health Stroke Scale (NIHSS) score, longer time to recanalization, lower platelet count and a higher glucose level are associated with HT [14].

**Figure 6.8**

Petechial hemorrhage. Gyriform low signal in the right frontal lobe (*arrow*) on this GRE T2\* image corresponds to susceptibility from petechial hemorrhage in an acute infarct

**Figure 6.9**

Hemosiderin in chronic infarct. The low signal from the gyriform on this GRE T2\*-weighted image at the right frontal lobe is from hemosiderin in an old petechial bleed

Because T1-, T2-, and FLAIR-weighted images are insensitive at detecting acute blood products (deoxy-hemoglobin), GRE T2\* sequences should be used to detect hemorrhage in the acute stroke setting (Fig. 6.8). GRE T2\* sequences have increased sensitivity to blood breakdown products due to their paramagnetic properties. One study demonstrated GRE images to be as sensitive as CT at detecting parenchymal hemorrhage in acute strokes [15]. Another study observed that in detecting acute blood products, GRE T2\*-weighted images were more sensitive than T2-, FLAIR-, or echo planar T2-weighted images [16]. Some data suggest that microbleeds detected by susceptibility predict symptomatic hemorrhage following tissue plasminogen activator (t-PA) treatment [17].

As blood products evolve into methemoglobin, T1-weighted sequences become more sensitive at detecting blood products [18]. Chronic hemorrhages

are best detected on GRE T2\* images as areas of susceptibility (Fig. 6.9).

### 6.1.6 Conclusion

Conventional MRI can diagnose infarcts at all stages of temporal evolution but are most sensitive after the hyperacute stage (see Table 6.1). During the hyperacute stage, the predominant findings are loss of flow voids on T2-weighted images, FLAIR hyperintensity in affected vessels, and vascular enhancement. In the acute to chronic stage, FLAIR and T2 parenchymal abnormalities are evident and Wallerian degeneration develops. The subacute stage is also marked by parenchymal swelling followed by parenchymal enhancement. The detection of acute hemorrhagic infarct requires the use of a T2\* GRE susceptibility sequence since other conventional MRI sequences are not sensitive enough for acute bleeds.

**Table 6.1.** The appearance of arterial infarcts on conventional MRI

Stage	Conventional MR appearance	Evolution
Hyperacute (0–6 h)	T2 shows loss of signal flow void	Occurs within minutes of the infarct
	FLAIR shows vessel high signal	Occurs within minutes of the infarct
	GRE T2* shows blooming susceptibility	Occurs within minutes of the infarct
	T1 post-contrast shows arterial enhancement	Occurs at 2 hours and can last 7 days
	There are no reliable parenchymal findings for infarct at this stage	
Acute (6–24 hours)	Vascular abnormalities from the hyperacute stage persist	
	T2 and FLAIR show gyriform high signal and sulcal effacement	Appears by 24 h (90% sensitivity)
	T2 can show subcortical low signal	
	GRE T2* show gyriform susceptibility from petechial bleed	Can occur at any time in the acute to subacute stage
	No parenchymal enhancement is present	
Subacute (1 day to 2 weeks)	T2 and FLAIR show gyriform high signal and sulcal effacement from mass effect	Reaches a maximum at 3–5 days and decreases by 1 week. Rarely, "MR fogging" appears at 2 weeks
	T1 can show gyriform high signal from petechial bleed	Appears once methemoglobin develops
	T1 post-contrast shows arterial enhancement	Peaks at 1–3 days and resolves by 1 week
	T1 post-contrast shows meningeal enhancement	Peaks at 2–6 days and resolves by 1 week
	T1 post-contrast show parenchymal enhancement as vessels recanalize	Can be seen at 2–3 days, consistently seen at 6 days and persists for 6–8 weeks
Chronic	T2 shows high signal from gliosis and Wallerian degeneration	Persists indefinitely
	Volume loss is present	Persists indefinitely
	T1 shows low signal from cavitation	Persists indefinitely
	GRE T2* shows low signal hemosiderin from petechial bleeds	Persists indefinitely

## 6.2 MR Angiogram and Stroke

Magnetic resonance angiography (MRA) is a set of vascular imaging techniques capable of depicting the extracranial and intracranial circulation. In the setting of acute stroke, these techniques are useful for determining stroke etiology and assessing vascular

flow dynamics. Specifically, they are used to evaluate the severity of stenosis or occlusion as well as collateral flow. A typical stroke protocol includes two-dimensional (2D) and/or three-dimensional (3D) time-of-flight (TOF) and contrast-enhanced MRA images through the neck and 3D TOF MRA images through the Circle of Willis. For dissection, a fat saturated pre-gadolinium axial T1 sequence through the neck is

added. This section discusses the major MRA techniques, including the advantages and disadvantages of each, as well as how MRA is used to evaluate the specific disease processes that lead to stroke.

### 6.2.1 Noncontrast MRA

MRA is broadly divided into noncontrast and contrast-enhanced techniques. Noncontrast MRA can be acquired with phase contrast (PC) or TOF techniques, and both can be acquired as 2D slabs or 3D volumes.

#### 6.2.1.1 TOF MRA

TOF MRA is a gradient echo sequence that depicts vascular flow by repeatedly applying a radio frequency (RF) pulse to a volume of tissue, followed by dephasing and rephasing gradients. Stationary tissues in this volume become saturated by the repeated RF pulses and have relatively low signal. By contrast, flowing blood in vessels has relatively increased signal because it continuously carries unsaturated spins into the imaging volume. The vessel contrast or flow-related enhancement is proportional to the velocity. Signal from venous blood is minimized by placing a saturation band above the imaging volume [19].

Two-dimensional TOF MRA is typically performed in the neck region with a relatively large flip angle (60°). Multiple sequential, 1-mm-thick axial slices are obtained. Blood flowing perpendicular to the multiple thin slices is well imaged because it is not exposed to enough RF pulses to become saturated. However, blood flowing in the imaging plane (in-plane flow) is exposed to more RF pulses and may become saturated and lose signal; this artifact can often be seen at the horizontal turns of the vertebral arteries as well as the petrous segments of the internal carotid arteries (Fig. 6.10) [19].

Three-dimensional TOF MRA is typically performed in the head region with a smaller flip angle (20°). A volume of tissue covering the skull base to the Circle of Willis is obtained and then divided into 1-mm-thick slices using an additional phase encoding step [20]. While the smaller flip angle reduces saturation artifacts, any flowing blood that remains

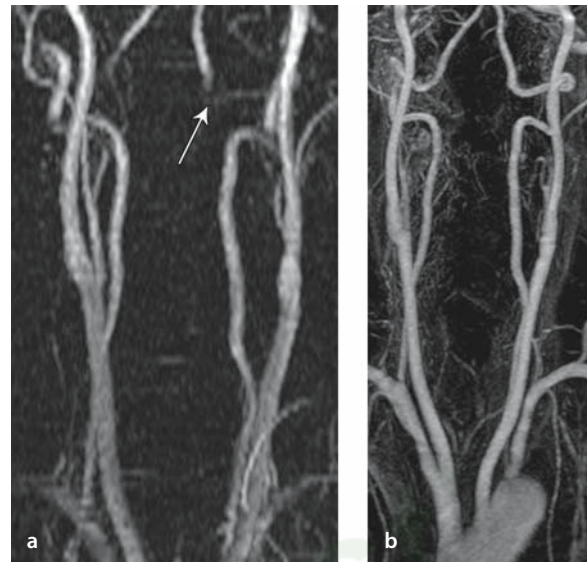


Fig. 6.10 a, b

Normal neck MRA. **a** MIP image of 2D TOF of the neck shows artifactual signal loss at the horizontal turn of the left vertebral artery (*arrow*). **b** This area has normal flow on MIP images from the contrast-enhanced MRA. The contrast-enhanced MRA gives excellent depiction of the origins of the neck vessels

in the imaging volume for long enough is exposed to multiple RF pulses and can artifactually lose signal. This signal loss is usually seen in the distal Circle of Willis vessels (Fig. 6.11). The smaller flip angle also decreases the background saturation. Typically, a ramped flip angle is used to minimize vascular saturation effects while maximizing the suppression of the background signal. Magnetization transfer is additionally applied in 3D TOF MRA to further decrease the background signal.

Compared with 2D TOF, the 3D TOF technique has better spatial resolution, a better signal-to-noise ratio and less intravoxel dephasing, but it is more limited by the vascular saturation artifact and therefore can cover only a small volume. A hybrid technique between 2D and 3D TOF known as MOTSA (multiple overlapping thin slab acquisition) acquires partially overlapping thin 3D volumes. The ends of the 3D volume have saturation artifact and are discarded while

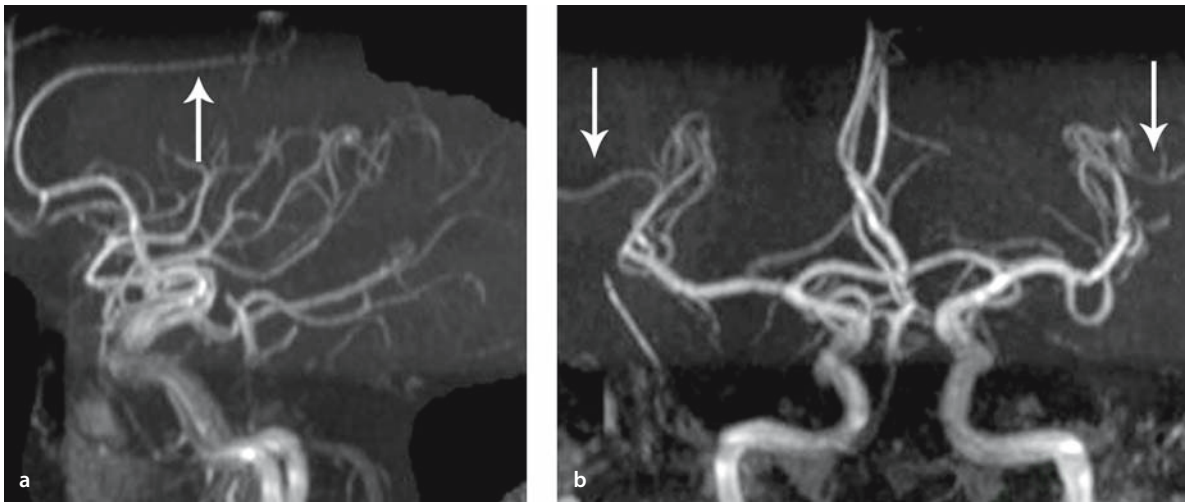
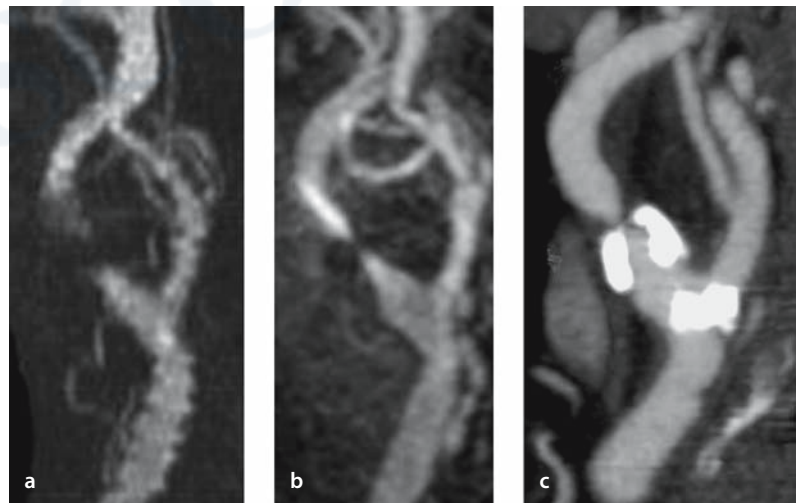


Fig. 6.11 a, b

Normal 3D TOF MRA of the head. Segmented MIP images from a frontal (a) and lateral (b) projection show normal vessels with decreased flow-related enhancement in the distal anterior cerebral artery (ACA) (arrow in a) and distal MCA vessels (arrows in b)

Fig. 6.12 a–c

Internal carotid artery (ICA) stenosis. a Time-of-flight (TOF) MRA shows a segment of signal loss at the proximal ICA. b The length of this focal signal loss is overestimated when compared with contrast-enhanced MRA. c This could represent stenosis or occlusion, but was shown to be a high-grade stenosis on CT angiogram



central portions are assembled into a single MRA. MOTSA has higher spatial resolution than 2D TOF while covering a larger area than 3D TOF MRA, because it is less susceptible to saturation artifact.

TOF MRA, especially 2D TOF, is also vulnerable to artifactual signal loss from flow turbulence. This

causes phase dispersion so that the rephasing gradient is unable to generate a strong echo. This artifact can be seen at vessel bifurcation points or distal to stenoses and can result in overestimates of the degree or length of vascular stenoses (Fig. 6.12).



**Fig. 6.13 a,b**

TOF MRA artifact. **a** Blood (methemoglobin) in the pre-pontine cistern has high signal on the TOF MRA because the signal from substances with a short T1 is not adequately suppressed. **b** On the MIP images, this high signal obscures portions of the basilar artery and left posterior cerebral artery

TOF MRA can have artifact from poor background suppression. Signal from stationary tissues are in theory suppressed with repeated RF pulses, but substances with a short T1, such as fat or methemoglobin in hematomas, are not usually fully saturated. Consequently, these substances demonstrate high signal on TOF MRA and can mimic areas of flow or obscure

vessels (Fig. 6.13). This artifact can sometimes be overcome by segmenting out areas of high signal, and high fat signal can be reduced by setting the echo time (TE) to 2.3 or 6.9 ms, to place fat and water out of phase.

### 6.2.1.2 Phase-Contrast MRA

Phase-contrast MRA (PC MRA) is a gradient echo sequence that depicts blood flow by quantifying differences in the transverse magnetization between stationary and moving tissue [19]. Following a RF pulse, pairs of symmetric but opposed phase encoding gradients are applied in one direction within the imaging volume; the first gradient dephases and the second rephases the transverse magnetization. Stationary tissues have no net change in phase because they experience equal but opposite magnetic field environments during the dephasing and then the rephasing gradients. Moving blood, however, experiences different magnetic field environments as each gradient is applied. The spins in moving blood acquire a phase shift during the dephasing pulse, which is not completely reversed during the rephasing pulse. The net phase shift, either positive or negative, determines direction of flow, and the amount of phase shift (in degrees) is proportional to the velocity or magnitude of blood flow.

PC MRA is acquired in three orthogonal directions, and the direction of flow is depicted as a relatively high or low signal against a gray background (Fig. 6.14). Orthogonal maps can also be combined to form an overall flow-related enhancement map without directionality. Like TOF MRA, PC MRA can be obtained with 2D or 3D techniques. Clinically, PC MRA is used to evaluate intracranial collateral flow distal to a stenosis.

An artifact unique to PC MRA is that phase shifts exceeding  $180^\circ$  are interpreted as slow flow in the opposite direction. This aliasing artifact leads to incorrect determination of flow direction. In order to avoid this, a velocity encoding parameter (VENC) is selected which represents the maximum expected flow velocity in the imaging volume. This value adjusts the strength of the bipolar gradients to prevent phase shifts from exceeding  $180^\circ$ .

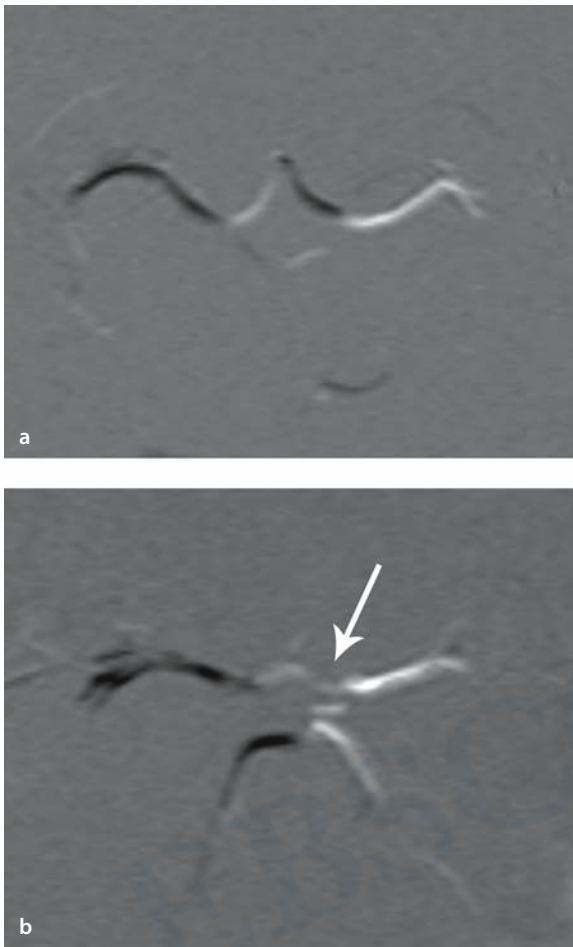


**Fig. 6.14 a, b**

Normal and abnormal phase-contrast MRA (PC MRA) of the circle of Willis. **a** Normal 2D PC MRA with direction encoding in the right/left direction (vessel is bright if flowing right to left and dark if flowing left to right). Normally the signal in the A1 branch is opposite that in the M1 branches. **b** Two-dimensional PC MRA from a 4-year-old with severe stenosis in the left internal carotid artery (ICA) shows retrograde flow in the left A1 (arrow) via the anterior communicating artery (ACoA). The left A1 and M1 therefore have the same high signal

PC MRA has several advantages over TOF MRA. As mentioned above, PC MRA can demonstrate flow direction. Also, since PC MRA shows only moving tissues, stationary tissues with short T1 such as fat or methemoglobin do not demonstrate high signal. Another advantage is that PC MRA can image very slowly moving blood since it does not suffer the saturation effects of TOF imaging. Finally, PC MRA can be obtained after i.v. gadolinium administration without image degradation because PC MRA does not rely on T1 values to generate the MRA image. Following contrast, TOF MRA is usually limited because gadolinium shortens the T1 and veins become hyperintense.

The major disadvantage of PC MRA is that it uses a longer TE than TOF MRA. This results in increased intravoxel dephasing and signal loss around stenoses and areas of turbulence. Also, 3D PC MRA has similar spatial resolution but is a longer sequence compared to 3D TOF MRA and is therefore more susceptible to motion artifacts. Consequently, 3D TOF MRA is usually employed to image the head. However, if there is concern that a subacute clot may mimic flow-related enhancement, 3D PC MRA should be performed. Also, because 3D TOF MRA cannot determine flow direction, 2D PC MRA (a much shorter sequence compared to 3D PC MRA) is frequently used to assess collateral retrograde flow in the anterior or posterior communicating arteries in association with severe internal carotid artery (ICA) stenosis or to assess retrograde flow in the basilar artery due to severe stenosis.

In the neck, TOF techniques are preferred over PC techniques due to the latter's longer scan times, which are needed to provide the same coverage and spatial resolution. Two-dimensional TOF MRA provides superior flow-related enhancement and allows coverage of the entire neck. Compared to 2D TOF MRA, 3D TOF MRA provides superior spatial resolution and is less susceptible to phase dispersion artifacts, but it is more susceptible to saturation effects and cannot cover a large area. Three-dimensional TOF techniques are therefore used to delineate the bifurcation only. Two-dimensional PC techniques are used to evaluate flow direction in the vertebral arteries when subclavian steal is suspected. Also, since

compared to TOF, 2D PC techniques are more sensitive to the detection of very slow flow, they can be used to differentiate high-grade stenosis with a string sign from occlusion.

### 6.2.2 Contrast-Enhanced MRA

Contrast-enhanced MRA (CE MRA) is performed with a rapid, short repetition time (TR, 10 ms) gradient echo sequence following an i.v. bolus of gadolinium. The gadolinium shortens the T1 to less than 10 ms so that opacified vessels are hyperintense. Background tissues, including normally T1-hyperintense structures such as fat and methemoglobin in hematomas, have low signal because they have intrinsic T1 relaxation times of much greater than 10 ms [19].

CE MRA is usually obtained from the arch to the skull base in the coronal plane and is often obtained with a first-pass technique (Fig. 6.10). This requires obtaining the MRA during peak arterial enhancement to avoid venous enhancement. The timing of this arterial phase can be determined by a test bolus or by automatic bolus detection. k-space is filled during peak arterial enhancement in order to maximize image contrast. Another technique known as time-resolved CE MRA acquires the MRA and fills k-space before, during, and after the arterial bolus. This does not require synchronization of the MRA with the injection. In theory, this technique can depict flow dynamics but is limited by the trade-off between temporal and spatial resolution [19].

CE MRA is a reliable modality to image neck vessels but can have poor signal-to-noise ratio at the edge of the imaging volume or have respiratory motion artifact. Respiratory motion artifact limits adequate visualization of the major vessel origins off the arch as well as the origins of the right common, right subclavian, and bilateral vertebral arteries.

CE MRA has several advantages over noncontrast MRA (i.e., PC and TOF MRA): CE MRA can cover a much larger area of anatomy (from the arch to the skull base) in a much shorter acquisition time and is less susceptible to patient motion. CE MRA also has a greater signal-to-noise ratio and less dephasing from turbulence and does not suffer signal loss from satu-

ration effects. CE MRA images the contrast within a vessel lumen and is therefore a more anatomic evaluation, while noncontrast MRA depicts physiology, and anatomy must be inferred from blood flow. This can be misleading when a vessel is not seen on TOF techniques due to reversal of flow or very slow flow (Fig. 6.15).

The disadvantages of CE MRA compared to noncontrast MRA is that the CE MRA data must be obtained during the narrow time window of arterial enhancement and cannot be repeated until the intravascular gadolinium agent is cleared. Thus improper timing (scanning too early or late) results in poor arterial enhancement and an inadequate study that cannot immediately be repeated. Also, the spatial resolution of CE techniques is inferior to that of TOF techniques, and contrast MRA is also minimally invasive as it typically requires a 20-ml power injection of gadolinium contrast at 2 ml/s.

In clinical practice, CE MRA is routinely used to image the great vessel origins and the neck. In general, it does not overestimate carotid bifurcation and other stenoses as much as TOF techniques because it is less susceptible to dephasing from turbulence and does not suffer signal loss from saturation effects. However, many institutions continue to image the neck with both CE and TOF techniques. Due to poorer spatial resolution, CE MRA may underestimate carotid stenosis. TOF techniques are also useful when the arterial bolus is timed incorrectly and when there is unsuspected reversal of flow. For example, in Fig. 6.15, the left vertebral artery appears normal on the CE image and one would assume antegrade flow. However, the vessel is not seen on the 2D TOF flight images, suggesting retrograde flow with saturation of spins due to a superior saturation pulse.

A comparison of the MRA techniques and their typical clinical applications is presented in Table 6.2.

### 6.2.3 Image Processing

Noncontrast and contrast MRA can be post-processed as a maximum intensity projection (MIP) image. This technique first creates a 3D model of the vessels from the MRA raw data. A set of parallel rays is then drawn from the model and the highest inten-

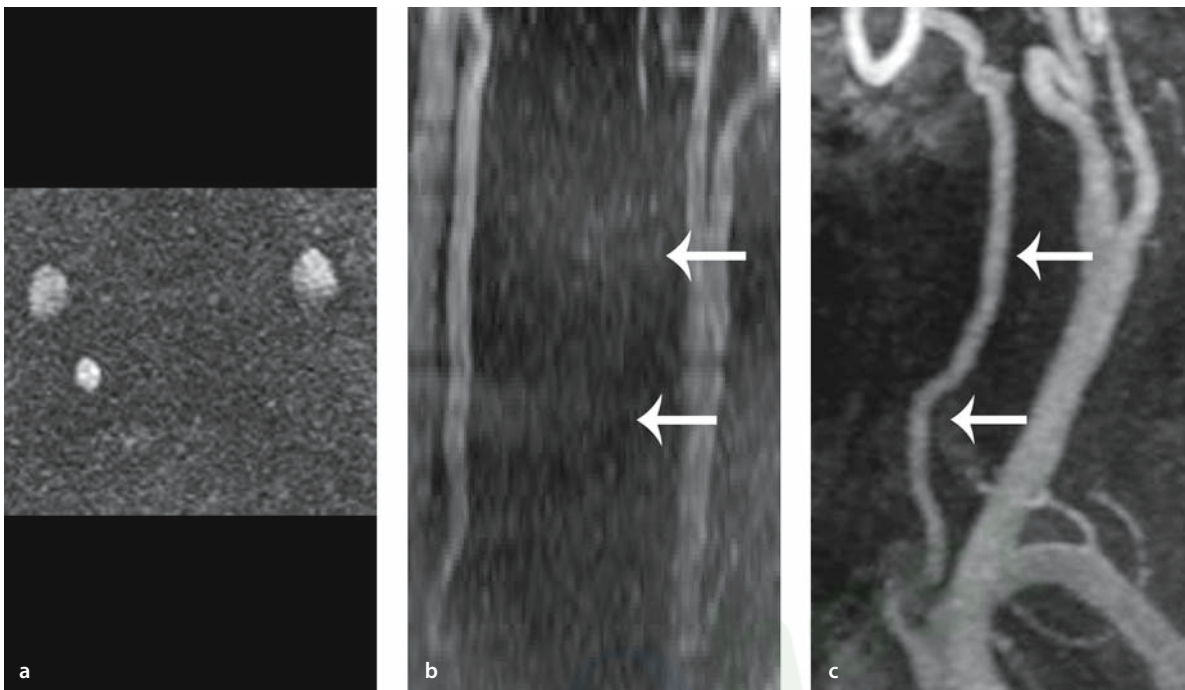


**Fig. 6.15 a–c**

Slow flow or subclavian steal syndrome. Two-dimensional TOF MRA source image (a) and MIP image of the TOF MRA (b) show absent flow and possible occlusion of the left vertebral artery (arrows in b). CE MRA (c), however, shows flow in this vessel (arrows). This discrepancy can occur from slow flow leading to signal saturation on 2D TOF or from reversed flow in subclavian steal syndrome

sity along each ray is projected to form a 2D MIP image. Multiple projections of the model are created from different vantage points so that viewing sequential MIP images gives the illusion of observing a rotating 3D MRA model.

#### 6.2.4 Extracranial Atherosclerosis and Occlusions

MRA of neck vessels is important in stroke management because extracranial atherosclerosis causes an estimated 20–30% of strokes. The North American Symptomatic Carotid Endarterectomy Trial (NASCET) trial demonstrated that carotid endarterectomy improves survival in symptomatic patients with carotid stenosis of 70–99% [21]. The Asymptomatic Carotid

Atherosclerosis Study also suggested that asymptomatic patients with a stenosis of 60% could benefit from endarterectomy [22]. Since then, multiple studies have evaluated the ability of CE and noncontrast MRA to distinguish between nonsurgical (<70%) and surgical (70–99%) stenoses.

CE MRA is generally accurate in evaluation of stenoses. A 2003 study comparing CE MRA and digital subtraction angiography (DSA) showed a sensitivity of 97% and specificity of 95% for stratifying nonsurgical from surgical stenoses [23]. However, a 2004 prospective study also comparing DSA and CE MRA showed a sensitivity of 93% and specificity of 81% for detecting severe stenosis [24]. This poorer performance of CE MRA was attributed to interobserver variability, and this study noted that using CE

**Table 6.2.** MRA techniques and applications. (*CE MRA* Contrast-enhanced MRA, *PC* phase contrast, *TOF* time of flight)

	Advantages	Disadvantages	Clinical applications
2D TOF	Is noninvasive	Typically overestimates vessel stenosis	Is used routinely as the “back up” MRA of the neck in case the CE MRA is suboptimal
	Can image slow flow	Has in-plane artifactual signal loss	is used routinely in MR venography
	Can image a large volume of tissue	Is susceptible to signal loss from flow turbulence	can sometimes suggest subclavian steal if combined with CE MRA
	Can be repeated if suboptimal	Has low spatial resolution	
	Can be obtained after contrast administration but is slightly degraded by venous signal	Has misregistration artifact on MIP reconstructions	
3D TOF	Is noninvasive	Can image only a small volume due to saturation artifact	Is used routinely to evaluate the circle of Willis to detect intracranial stenoses and occlusions
	Has high spatial resolution	Has poor background suppression; fat or blood may appear bright on the MRA	Can estimate carotid bifurcation stenoses
	Shows complex vascular flow	Cannot image slow flow because of saturation effects	
	Is less susceptible to intravoxel dephasing	Is time consuming and susceptible to patient motion	
	Can be repeated if suboptimal		
2D PC MRA	Can be obtained after contrast administration but is slightly degraded by venous signal		
	Is able to show the direction and magnitude of flow	Has low spatial resolution	Is used occasionally to determine collateral flow around the circle of Willis
	Does not show high signal artifact from fat or blood	Is more susceptible to turbulent dephasing than TOF MRA	Is used occasionally to determines subclavian steal and abnormal flow direction in the neck
	Can show very slow moving blood and helps differentiate occlusion from near occlusion	Can have aliasing artifact if an incorrect VENC is used	Can detect slow flow if near-occlusion is suspected
	Can be obtained after gadolinium administration	2D PC of the neck takes longer than 2D TOF of the neck with similar coverage	Is used occasionally in MR venography
	Can be repeated if suboptimal		
	2D PC of the circle of Willis is faster than 3D TOF or PC MRA		

Table 6.2. (continued)

	Advantages	Disadvantages	Clinical applications
3D PC MRA	Has high spatial resolution	Is time consuming; 3D TOF MRA is faster with similar spatial resolution	Is rarely used
CE MRA	Does not show high signal artifact from fat or blood		Used if intravascular clot will confuse 3D TOF MRA interpretation
	Is fast, thus minimizing patient motion artifact	Has lower spatial resolution than 3D TOF MRA	Is used routinely to evaluate stenoses and occlusions of the neck vessels and neck vessel origins at the aortic arch
	Is less susceptible to signal loss from flow turbulence	Occasionally underestimates stenosis	
	Has no saturation artifact	Must be obtained in arterial phase	
	Has good signal-to-noise ratio	Cannot be repeated until i.v. contrast has cleared	
	Images a large volume of tissue	Is minimally invasive, requiring rapid power injection of contrast	
	Does not show high signal artifact from fat or blood		
Accurate in estimating stenoses			
Helps differentiate occlusion from near-occlusion			

MRA alone would have misclassified 15% of cases and would have altered clinical decision-making in 6.0% of cases [24]. The authors concluded that this was a sufficiently low error rate to support use of CE MRA, but noted that catheter angiography was still the gold standard.

A 2003 study observed that stenoses measured by CE MRA and DSA are tightly correlated by a linear regression analysis ( $r=0.967$  with a 95% confidence interval of 2.8%) [25]. While this was true for the study overall, the study warned that stenosis measurements by a single CE MRA exam for an individual patient have a larger confidence interval and may not reliably discriminate between small increments of stenosis (e.g., between a 69% and 71% stenosis). Nevertheless, in most patients, CE MRA is accurate for stratifying stenoses into the broad categories of surgical versus nonsurgical lesions.

Some reports suggest that noncontrast MRA of the neck is less accurate than CE MRA in discriminating surgical from nonsurgical stenoses. One 2002 study comparing 2D and 3D TOF MRA to DSA reported that 23% of their patients would have received unindicated endarterectomies while another 33% would have been improperly denied endarterectomies had noncontrast MRA results been used alone [26]. Several studies from 1992 to 1994 also reported that 2D TOF MRA overestimated up to 48% of moderate stenoses, erroneously categorizing them as surgical lesions [27] and one study demonstrated that 2D TOF MRA has a sensitivity of 84% and specificity of 75% in differentiating surgical from nonsurgical stenoses [28]. However, a number of studies suggest that 3D TOF MRA has a sensitivity and specificity of grading carotid artery stenosis similar to those of CE MRA. One study demonstrated a sensitivity of 94%

and specificity of 85% for 3D TOF MRA in distinguishing surgical from nonsurgical stenoses [28]. Another study demonstrated Pearson correlation coefficients of 0.94 for CE MRA versus DSA, 0.95 for 3D TOF MRA versus DSA and 0.94 for CE MRA versus 3D TOF MRA [29]. Also, a 2003 meta-analysis combining 4 contrast and 17 noncontrast MRA studies published from 1994 to 2001 reported a pooled sensitivity of 95% and pooled specificity of 90% for MRA's ability to discriminate between stenoses greater than or equal to 70% [30].

In general, both noncontrast and CE MRA overestimate stenoses when compared with DSA, and this leads to a decrease in specificity. For noncontrast MRA, this is primarily related to signal loss from dephasing and saturation artifacts. Pixel exclusion on MIP images and motion degradation can also artifactually exaggerate the degree of stenosis on both noncontrast and CE MRA [24]. Nearly all studies evaluating MRA rely on DSA as a gold standard since this was used in the NASCET and ACAS trials. Some papers, however, question the accuracy of DSA in grading stenoses, pointing to underestimation of stenosis by DSA compared with 3D rotational catheter angiography [31, 32]. Some have suggested that the specificity measured on MRA studies may be falsely low from using a suboptimal gold standard [31].

Discriminating near occlusion from total occlusion is critical, as the former can indicate urgent surgery while the latter contraindicates surgical treatment. Several studies show that MRA has high sensitivity and specificity for making this differentiation [30, 33, 34]. El-Saden et al. [33], in a retrospective study using noncontrast and CE MRA together, reported a 92% sensitivity for detecting 37 total occlusions and a 100% sensitivity for detecting 21 near-occlusions [33]. A meta-analysis of both CE MRA and noncontrast MRA studies reported a pooled sensitivity of 98% and pooled specificity of 100% in differentiating high-grade stenosis from occlusion [30]. Other studies, however, do not report such high accuracies [35] and many practices still rely on DSA to differentiate definitively occlusion from near-occlusion.

### 6.2.5 Intracranial Atherosclerosis and Occlusions

In the setting of acute stroke, intracranial MRA can detect areas of stenosis and occlusion as well as determine collateral flow (Fig. 6.16). Defining the location of intracranial vessel pathology is clinically important since an estimated 38% of patients with acute strokes have arterial occlusion seen on DSA [36] (and distal clots are more likely than proximal clots to recanalize following tissue plasminogen activator (t-PA) [37]. As a result, proximal clots are treated more aggressively, sometimes using intra-arterial techniques. In the acute setting, localizing intracranial occlusions is often performed by CT angiogram, but MRA can also depict these findings (Fig. 6.17).

Several studies report that intracranial MRA has a variable reliability of detecting occlusion and stenoses in the acute stroke setting. A 1994 study of TOF MRA compared to DSA in stroke reported 100% sensitivity and 95% specificity for detecting intracranial occlusion [38], and another demonstrated 88% sensitivity and 97% specificity for detecting MCA lesions compared with DSA [39]. A 2002 study, however, showed that, with the addition of contrast to TOF MRA, 21% of vessels initially thought to be occluded on noncontrast TOF MRA were actually patent on CE TOF MRA [40]. Few studies have determined the clinical significance of these MRA findings in stroke, but a recent 2004 study using phase-contrast MRA in acute stroke showed that absent flow in the M1 segment can help predict infarct growth [41].

The degree of collateral flow seen on DSA is an independent radiologic predictor of favorable outcome following thrombolytic treatment [42]. TOF MRA, however, is limited in evaluation of collateral flow. One study found a negative predictive value as low as 53% for TOF MRA's ability to detect collateral flow when compared with transcranial Doppler [43]. A 2004 study showed that, on TOF MRA, prominence of distal PCA vessels ipsilateral to an M1 occlusion represents collateral blood flow via leptomeningeal vessels [44]. The significance of this finding remains uncertain.

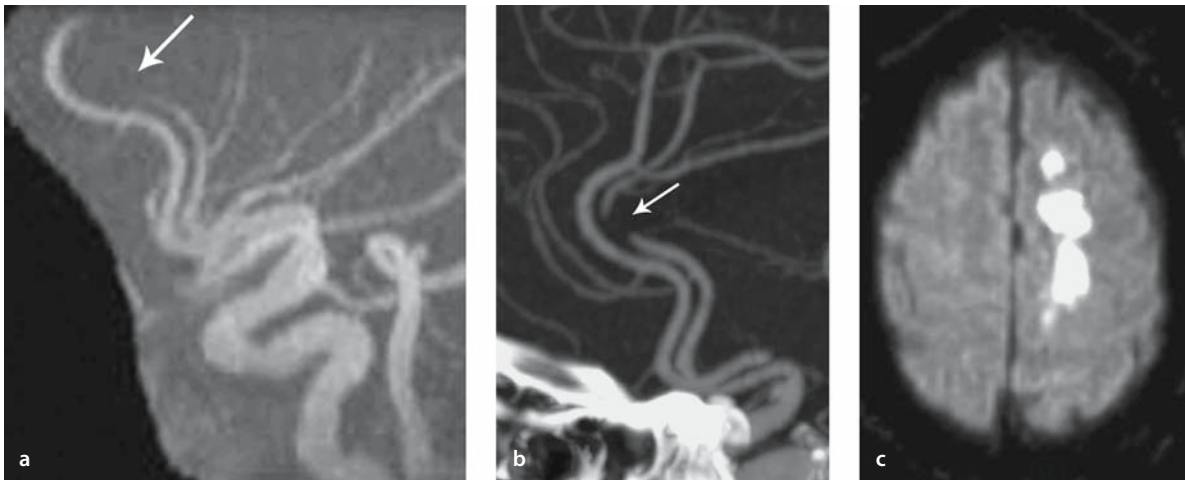


Fig. 6.16 a–c

Anterior cerebral artery occlusion and infarct. **a** MIP of 3D TOF MRA shows absent flow-related enhancement of the distal A2 segment of the left anterior cerebral artery (ACA, arrow). **b** This corresponds to a focal filling defect on CT angiography (CTA, arrow). Note that MRA cannot image the slow collateral flow in the distal left ACA. **c** Diffusion-weighted image (DWI) shows the left ACA territory infarct

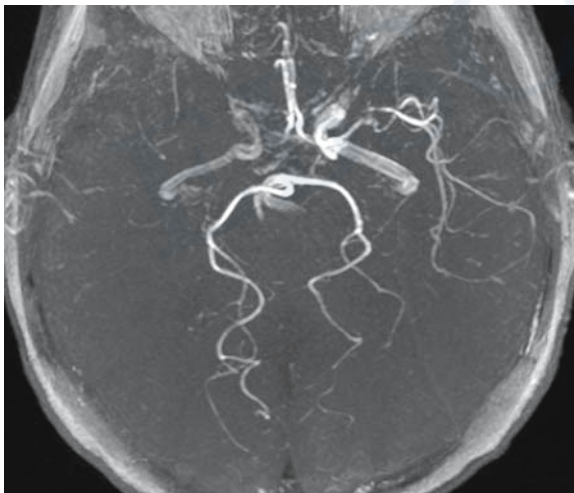


Figure 6.17

Right MCA occlusion. Three-dimensional TOF MRA MIP image shows absent flow-related enhancement in the right MCA from embolic occlusion. Note the decreased signal in the right petrous ICA from a saturation effect secondary to slow flow. There is also severe stenosis of the distal left MCA

## 6.2.6 Dissection

Vascular dissection is an important etiology of acute infarction, causing up to 20% of infarcts in young patients and an estimated 2.5% of infarcts in the overall population [45]. Dissection occurs when blood extends into the wall of a vessel through an intimal tear. This may occur in the extracranial or intracranial vessels, the carotid or vertebral arteries, and may be spontaneous or post-traumatic in etiology [46, 47]. Dissection most frequently occurs in the carotid artery as it enters the skull base and in the vertebral artery segment from C2 to the foramen magnum. Dissections cause stroke primarily through embolization rather than through flow limitation [48].

Acute dissections show luminal narrowing on MRA and a flap can occasionally appear as a linear low signal defect on MRA. The signal of the intramural blood follows that of parenchymal hematomas, but hemosiderin deposition is not typically seen. Once methemoglobin develops, the wall of the vessel appears hyperintense on fat-saturated T1-weighted images [49] (Fig. 6.18). Chronically, the vessel can occlude, recanalize, show pseudoaneurysms, or become dilated [50].

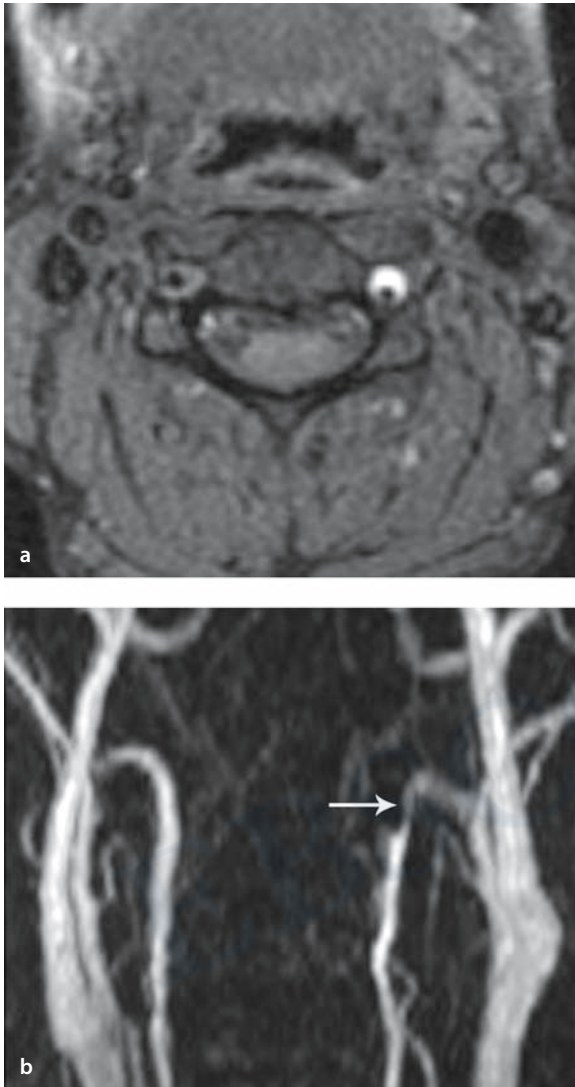


**Fig. 6.18 a, b**

Left vertebral artery dissection. **a** Axial T1 fat-saturated image of the neck shows a crescent of high signal at the left vertebral artery from intramural hemoglobin. **b** Contrast-enhanced MRA shows a narrowed left vertebral artery (arrow)

In a study of 19 internal carotid and five vertebral artery dissections, the MR appearance alone had an estimated 84% sensitivity and 99% specificity for diagnosing carotid dissections and a 60% sensitivity and 98% specificity for diagnosing vertebral artery dissection [51]. Noncontrast MRA (TOF) has low sensitivity (20%) for detecting vertebral artery dissection, but preliminary data suggest that CE MRA may improve the evaluation of vertebral artery dissection [52]. Recently, case reports of false-negatives have been reported for CE MRA in diagnosing dissection [53].

## 6.2.7 Other Infarct Etiologies

MRA can help determine other etiologies of arterial infarct, including moyo moyo disease, vasculitis, and fibromuscular dysplasia.

### 6.2.7.1 Moyo Moyo

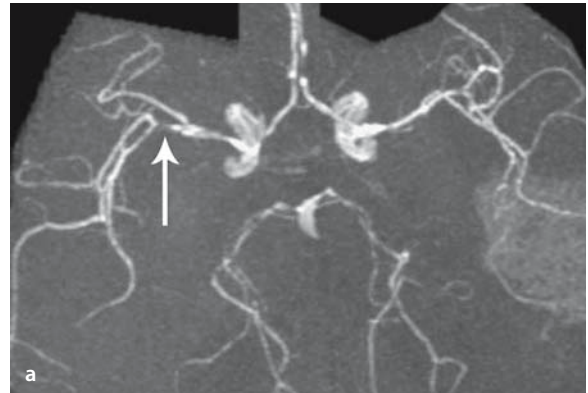
The term moyo moyo refers to primary moyo moyo disease and moyo moyo pattern, associated with an underlying disease such as atherosclerosis or radiation therapy. There is an increased incidence of primary moyo moyo disease in Asians and in patients with neurofibromatosis or sickle cell disease. Pathologically, there is a progressive occlusive vasculopathy of the supraclinoid internal carotid artery with extension into the proximal anterior and middle cerebral arteries associated with characteristic dilated prominent collateral vessels. Pediatric patients with moyo moyo disease tend to develop symptoms from acute infarction while adults with moyo moyo disease more frequently present with symptoms from intracranial hemorrhage into the deep gray nuclei. MRA can depict stenoses and occlusion of the internal carotid, middle cerebral, and anterior cerebral arteries (Fig. 6.19) [54, 55], and the estimated sensitivity and specificity of MRA in diagnosing moyo moyo disease in one study of 26 patients were 73% and 100% respectively [56]. Furthermore, one recent study reported that MRA depiction of moyo moyo collaterals in patients with sickle cell anemia was correlated with future cerebrovascular events [57]. MRA is also frequently used in planning vascular by-pass surgery and following response to treatment.

**Figure 6.19**

Moya moya disease. Three-dimensional TOF MRA shows decreased flow-related enhancement in the left ICA at the skull base. There is high-grade stenosis or occlusion at the left supraclinoid ICA in this patient with sickle cell anemia

### 6.2.7.2 Vasculitis

Vasculitis affecting the central nervous system (CNS) represents a heterogeneous group of inflammatory diseases that may be idiopathic or associated with autoimmune diseases, infections, drug exposure, radiation or cancer. Vessel walls are infiltrated by inflammatory cells, and there is increased vasomotor reactivity related to the release of neuropeptides. These properties lead to vessel narrowing. There is also loss of normal endothelial anticoagulant properties and vessels have increased susceptibility to thrombosis. Consequently, patients with vasculitis develop ischemic and thrombotic infarctions. There is also altered wall competence, which can result in dissection or vessel wall disruption with intracranial hemorrhage. MRA is clinically used to screen for vasculitis, but is less sensitive than DSA (Fig. 6.20). One study of 14 patients with suspected vasculitis reported that MRA could detect distal stenoses in vasculitis with a sensitivity of 62–79% and a specificity of 83–87% when compared with a DSA gold standard [58].

**Fig. 6.20 a,b**

Vasculitis. **a** MIP of 3D TOF MRA shows scattered areas of narrowing in the right MCA (*arrow*), bilateral posterior cerebral artery (PCA), and anterior cerebral artery (ACA) in this patient with primary CNS vasculitis. **b** MIP from CT angiogram also shows scattered vessel narrowing, especially at the right MCA (*arrow*)

### 6.2.7.3 Fibromuscular Dysplasia

Fibromuscular dysplasia (FMD) is an uncommon idiopathic vasculopathy causing stenoses most often in the renal and internal carotid arteries, and patients with FMD of the neck vessels can present with infarcts or transient ischemic attacks. MRA in FMD can show alternating areas of stenosis (Fig. 6.21) but one study noted that 2D TOF MRA is limited in evaluation of FMD, as slice misregistration artifacts can mimic alternating stenoses [59]. In practice, MRA is useful in distinguishing FMD from vessel dissection or hypoplasia [60].

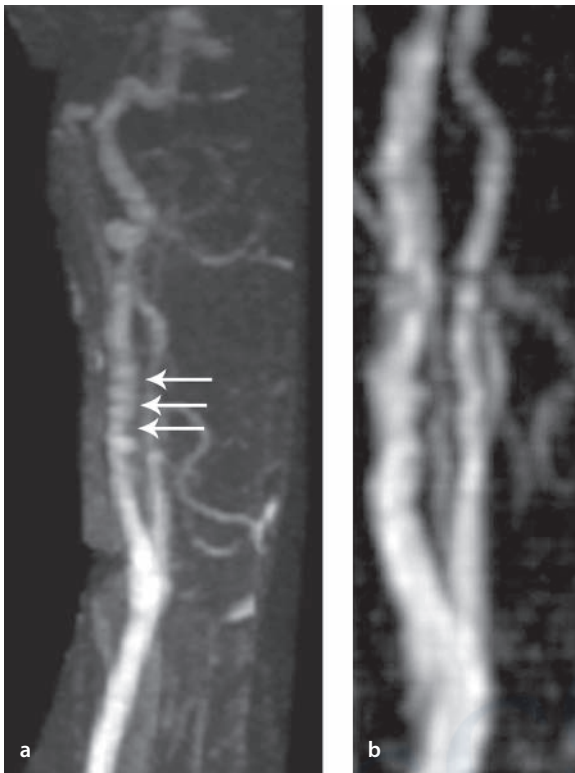


**Fig. 6.21 a,b**

Fibromuscular dysplasia. **a** CE MRA of the left internal carotid artery shows alternating stenoses (*arrows*) in this patient with fibromuscular dysplasia. **b** 2D TOF MIP image also demonstrates the stenoses but these can be confused with slice misregistration artifacts

### 6.2.8 Venous Infarct

Venous occlusion can lead to infarct through a reduction in cerebral blood flow. Venous infarcts are under-recognized and tend to develop into a hemorrhage [61]. Parenchymal findings on MR include imaging cerebral swelling, venous infarctions, and in-

tracranial hemorrhage. The MR appearance of intravascular clot is variable depending on the age of thrombus and the degree of residual flow. In general, methemoglobin demonstrates hyperintensity on T1-weighted images and there is usually the absence of a flow void on T2-weighted images.

MR venography greatly aids in diagnosing cerebral venous thrombosis and in determining the extent of thrombosis. Typically, a 2D TOF sequence is obtained in the coronal plane [62]. If flow-related enhancement is not seen within a sinus, there should be a high suspicion of sinus thrombosis (Fig. 6.22). However, MRV must be interpreted alongside standard MR sequences because the absence of flow-related enhancement can also be seen in atretic sinuses, in regions of complex flow due to complex geometry or where there is in-plane flow [63]. In addition, T1 hyperintense clot can be confused with flow-related enhancement on TOF techniques but the flow-related enhancement usually has higher signal intensity. Preliminary data also support the use of first-pass contrast-enhanced venography [64].

### 6.2.9 Conclusion

In the setting of acute stroke, MRA is useful for determining the severity of stenosis, vascular occlusion, and collateral flow. CE MRA and 3D TOF techniques have relatively high sensitivity and specificity in differentiating surgical from nonsurgical carotid stenoses. Three-dimensional TOF MRA is quite sensitive and specific for the evaluation of intracranial proximal stenoses and occlusions. Two-dimensional PC MRA is useful for determining collateral flow patterns in the circle of Willis. MRA is also useful in the determination of stroke etiologies such as dissection, fibromuscular dysplasia, vasculitis, and *moya moya*. Currently, MRA is relatively insensitive to the detection of stenoses in distal intracranial vessels but this detection will improve with new MR hardware and software.

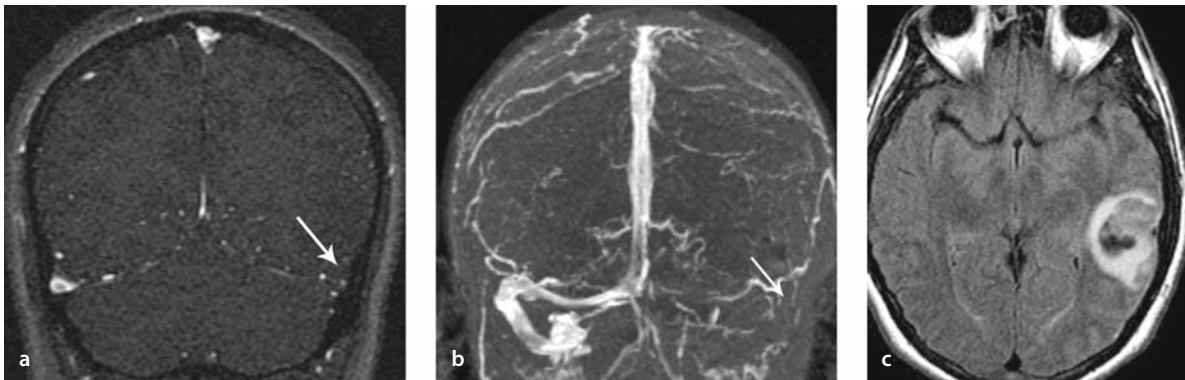


Fig. 6.22 a–c

Venous thrombus and venous infarct. 2D TOF MRV (a) and MIP image of the MR venogram (b) show absent flow in the left transverse sinus corresponding to thrombus (arrow). c FLAIR image shows high and low signal at the posterior left temporal lobe corresponding to hemorrhagic infarct

## References

1. Yuh WT et al (1991) MR imaging of cerebral ischemia: findings in the first 24 hours. *Am J Neuroradiol* 12(4):621–629
2. Maeda M et al (2001) Time course of arterial hyperintensity with fast fluid-attenuated inversion-recovery imaging in acute and subacute middle cerebral arterial infarction. *J Magn Reson Imaging* 13(6):987–990
3. Flacke S et al (2000) Middle cerebral artery (MCA) susceptibility sign at susceptibility-based perfusion MR imaging: clinical importance and comparison with hyperdense MCA sign at CT. *Radiology* 215(2):476–482
4. Shimosegawa E et al (1993) Embolic cerebral infarction: MR findings in the first 3 hours after onset. *Am J Roentgenol* 160(5):1077–1082
5. Perkins CJ et al (2001) Fluid-attenuated inversion recovery and diffusion- and perfusion-weighted MRI abnormalities in 117 consecutive patients with stroke symptoms. *Stroke* 32(12):2774–2781
6. Ida M et al (1994) Subcortical low intensity in early cortical ischemia. *Am J Neuroradiol* 15(7):1387–1393
7. Ricci PE et al (1999) A comparison of fast spin-echo, fluid-attenuated inversion-recovery, and diffusion-weighted MR imaging in the first 10 days after cerebral infarction. *Am J Neuroradiol* 20(8):1535–1542
8. Asato R, Okumura R, Konishi J (1991) “Fogging effect” in MR of cerebral infarct. *J Comput Assist Tomogr* 15(1):160–162
9. Crain MR et al (1991) Cerebral ischemia: evaluation with contrast-enhanced MR imaging. *Am J Neuroradiol* 12(4):631–639
10. Kuhn MJ, Mikulis DJ, Ayoub DM, Kosofsky BE, Davis KR, Taveras JM (1989) Wallerian degeneration after cerebral infarction: evaluation with sequential MR imaging. *Radiology* 172(1):179–182
11. Boyko OB et al (1992) Non-heme mechanisms for T1 shortening: pathologic, CT, and MR elucidation. *Am J Neuroradiol* 13(5):1439–1445
12. Hornig CR, Dorndorf W, Agnoli AL (1986) Hemorrhagic cerebral infarction – a prospective study. *Stroke* 17(2):179–185
13. Hakim AM, Ryder-Cooke A, Melanson D (1983) Sequential computerized tomographic appearance of strokes. *Stroke* 14(6):893–897
14. Kidwell CS et al (2002) Predictors of hemorrhagic transformation in patients receiving intra-arterial thrombolysis. *Stroke* 33(3):717–724
15. Hermier M et al (2001) MRI of acute post-ischemic cerebral hemorrhage in stroke patients: diagnosis with T2\*-weighted gradient-echo sequences. *Neuroradiology* 43(10):809–815
16. Lin DD et al (2001) Detection of intracranial hemorrhage: comparison between gradient-echo images and b(0) images obtained from diffusion-weighted echo-planar sequences. *Am J Neuroradiol* 22(7):1275–1281
17. Hermier M, Nighoghossian N. Contribution of susceptibility-weighted imaging to acute stroke assessment. *Stroke* 35(8):1989–1994
18. Bradley WG Jr (1993) MR appearance of hemorrhage in the brain. *Radiology* 189(1):15–26
19. Jewells V, Castillo M (2003) MR angiography of the extracranial circulation. *Magn Reson Imaging Clin North Am* 11(4):585–597, vi

20. Sohn CH, Sevick RJ, Frayne R (2003) Contrast-enhanced MR angiography of the intracranial circulation. *Magn Reson Imaging Clin North Am* 11(4):599–614
21. Barnett HJ et al (1998) Benefit of carotid endarterectomy in patients with symptomatic moderate or severe stenosis. North American Symptomatic Carotid Endarterectomy Trial Collaborators. *N Engl J Med* 339(20):1415–1425
22. Executive Committee for the Asymptomatic Carotid Atherosclerosis Study (1995) Endarterectomy for asymptomatic carotid artery stenosis. *J Am Med Assoc* 273(18):1421–1428
23. Alvarez-Linera J et al (2003) Prospective evaluation of carotid artery stenosis: elliptic centric contrast-enhanced MR angiography and spiral CT angiography compared with digital subtraction angiography. *Am J Neuroradiol* 24(5):1012–1019
24. U-King-Im JM, Trivedi RA, Graves MJ et al (2004) Contrast-enhanced MR angiography for carotid disease: diagnostic and potential clinical impact. *Neurology* 62(8):1282–1290
25. Hathout GM, Duh MJ, El-Saden SM (2003) Accuracy of contrast-enhanced MR angiography in predicting angiographic stenosis of the internal carotid artery: linear regression analysis. *Am J Neuroradiol* 24(9):1747–1756
26. Wardlaw JM et al (2002) Interobserver variability of magnetic resonance angiography in the diagnosis of carotid stenosis – effect of observer experience. *Neuroradiology* 44(2):126–132
27. Stark DWB (1999) *Magnetic resonance imaging*. Elsevier, New York
28. Patel MR et al (1995) Preoperative assessment of the carotid bifurcation. Can magnetic resonance angiography and duplex ultrasonography replace contrast arteriography? *Stroke* 26(10):1753–1758
29. Nederkoorn PJ et al (2003) Carotid artery stenosis: accuracy of contrast-enhanced MR angiography for diagnosis. *Radiology* 228(3):677–682
30. Nederkoorn PJ, van der Graaf Y, Hunink MG (2003) Duplex ultrasound and magnetic resonance angiography compared with digital subtraction angiography in carotid artery stenosis: a systematic review. *Stroke* 34(5):1324–1332
31. Elgersma OE et al (2000) Multidirectional depiction of internal carotid arterial stenosis: three-dimensional time-of-flight MR angiography versus rotational and conventional digital subtraction angiography. *Radiology* 216(2):511–516
32. Elgersma OE et al (1999) Maximum internal carotid arterial stenosis: assessment with rotational angiography versus conventional intraarterial digital subtraction angiography. *Radiology* 213(3):777–783
33. El-Saden SM et al (2001) Imaging of the internal carotid artery: the dilemma of total versus near total occlusion. *Radiology* 221(2):301–308
34. Heiserman JE et al (1992) Carotid artery stenosis: clinical efficacy of two-dimensional time-of-flight MR angiography. *Radiology* 182(3):761–768
35. Modaresi KB et al (1999) Comparison of intra-arterial digital subtraction angiography, magnetic resonance angiography and duplex ultrasonography for measuring carotid artery stenosis. *Br J Surg* 86(11):1422–1426
36. Furlan A et al (1999) Intra-arterial prourokinase for acute ischemic stroke. The PROACT II study: a randomized controlled trial. *Prolyse in acute cerebral thromboembolism*. *J Am Med Assoc* 282(21):2003–2011
37. Del Zoppo GJ et al (1992) Recombinant tissue plasminogen activator in acute thrombotic and embolic stroke. *Ann Neurol* 32(1):78–86
38. Stock KW et al (1995) Intracranial arteries: prospective blinded comparative study of MR angiography and DSA in 50 patients. *Radiology* 195(2):451–456
39. Korogi Y et al (1994) Intracranial vascular stenosis and occlusion: diagnostic accuracy of three-dimensional, Fourier transform, time-of-flight MR angiography. *Radiology* 193(1):187–193
40. Yang JJ et al (2002) Comparison of pre- and postcontrast 3D time-of-flight MR angiography for the evaluation of distal intracranial branch occlusions in acute ischemic stroke. *Am J Neuroradiol* 23(4):557–567
41. Liu Y et al (2004) Acute ischemic stroke: predictive value of 2D phase-contrast MR angiography—serial study with combined diffusion and perfusion MR imaging. *Radiology* 231(2):517–527
42. Kucinski T et al (2003) Collateral circulation is an independent radiological predictor of outcome after thrombolysis in acute ischaemic stroke. *Neuroradiology* 45(1):11–18
43. Hoksbergen AW et al (2003) Assessment of the collateral function of the circle of Willis: three-dimensional time-of-flight MR angiography compared with transcranial color-coded duplex sonography. *Am J Neuroradiol* 24(3):456–462
44. Uemura A et al (2004) Prominent laterality of the posterior cerebral artery at three-dimensional time-of-flight MR angiography in M1-segment middle cerebral artery occlusion. *Am J Neuroradiol* 25(1):88–91
45. Provenzale JM (1995) Dissection of the internal carotid and vertebral arteries: imaging features. *Am J Roentgenol* 165(5):1099–1104
46. Shin JH et al (2000) Vertebral artery dissection: spectrum of imaging findings with emphasis on angiography and correlation with clinical presentation. *Radiographics* 20(6):1687–1696
47. Fisher CM, Ojemann RG, Roberson GH (1978) Spontaneous dissection of cervico-cerebral arteries. *Can J Neurol Sci* 5(1):9–19
48. Benninger DH et al (2004) Mechanism of ischemic infarct in spontaneous carotid dissection. *Stroke* 35(2):482–485
49. Ozdoba C, Sturzenegger M, Schroth G (1996) Internal carotid artery dissection: MR imaging features and clinical-radiologic correlation. *Radiology* 199(1):191–198
50. Mokri B et al (1986) Spontaneous dissection of the cervical internal carotid artery. *Ann Neurol* 19(2):126–138

51. Levy C et al (1994) Carotid and vertebral artery dissections: three-dimensional time-of-flight MR angiography and MR imaging versus conventional angiography. *Radiology* 190(1):97-103
52. Leclerc X et al (1999) Preliminary experience using contrast-enhanced MR angiography to assess vertebral artery structure for the follow-up of suspected dissection. *Am J Neuroradiol* 20(8):1482-1490
53. Khan R, Smith JK, Castillo M (2002) False-negative contrast MRA in the setting of carotid artery dissection. *Emerg Radiol* 9(6):320-322
54. Yamada I, Matsushima Y, Suzuki S (1992) Moyamoya disease: diagnosis with three-dimensional time-of-flight MR angiography. *Radiology* 184(3):773-778
55. Yamada I et al (2001) High-resolution turbo magnetic resonance angiography for diagnosis of Moyamoya disease. *Stroke* 32(8):1825-1831
56. Yamada I, Suzuki S, Matsushima Y (1995) Moyamoya disease: comparison of assessment with MR angiography and MR imaging versus conventional angiography. *Radiology* 196(1):211-2128
57. Steen RG et al (2003) Brain imaging findings in pediatric patients with sickle cell disease. *Radiology* 228(1):216-225
58. Demaerel P et al (2004) Magnetic resonance angiography in suspected cerebral vasculitis. *Eur Radiol* 14(6):1005-1012
59. Heiserman JE et al (1992) MR angiography of cervical fibromuscular dysplasia. *Am J Neuroradiol* 13(5):1454-1457
60. Furie DM, Tien RD (1994) Fibromuscular dysplasia of arteries of the head and neck: imaging findings. *Am J Roentgenol* 162(5):1205-1209
61. Tsai FY et al (1995) MR staging of acute dural sinus thrombosis: correlation with venous pressure measurements and implications for treatment and prognosis. *Am J Neuroradiol* 16(5):1021-1029
62. Liauw L et al (2000) MR angiography of the intracranial venous system. *Radiology* 214(3):678-682
63. Ayanzen RH et al (2000) Cerebral MR venography: normal anatomy and potential diagnostic pitfalls. *Am J Neuroradiol* 21(1):74-78
64. Farb RI et al (2003) Intracranial venous system: gadolinium-enhanced three-dimensional MR venography with auto-triggered elliptic centric-ordered sequence-initial experience. *Radiology* 226(1):203-209